Microwave Design Optimization Exploiting Adjoint Sensitivity

Slawomir Koziel, Leifur Leifsson and Stanislav Ogurtsov
Engineering Optimization & Modeling Center, School of Science and Engineering, Reykjavik University, Reykjavik, Iceland

Keywords: Computer-aided Design (CAD), Simulation-driven Design, Microwave Design Optimization, Electromagnetic Simulation, Adjoint Sensitivity.

Abstract: Adjustment of geometry and material parameters is an important step in the design of microwave devices and circuits. Nowadays, it is typically performed using high-fidelity electromagnetic (EM) simulations, which might be a challenging and time consuming process because accurate EM simulations are computationally expensive. In particular, design automation by employing an EM solver in an numerical optimization algorithm may be prohibitive. Recently, adjoint sensitivity techniques become available in commercial EM simulation software packages. This makes it possible to speed up the EM-driven design optimization process either by utilizing the sensitivity information in conventional, gradient-based algorithms or by combining it with surrogate-based approaches. In this paper, we review several recent methods and algorithms for microwave design optimization using adjoint sensitivity. We discuss advantages and disadvantages of these techniques and illustrate them through numerical examples.

1 INTRODUCTION

Contemporary microwave engineering heavily relies on electromagnetic (EM) simulation. EM simulation is not only used for design verification but in the design process itself, i.e., to adjust geometry and/or material parameters of the structure under consideration. Unfortunately, accurate EM simulation is CPU intensive. A way to speed it up is parallelization (OpenMP, MPI, GPU) or distributed computing. However, the bottleneck in EM-simulation-based optimization remains to be the large number of EM simulations required by conventional optimization algorithms. Another problem is related to the numerical noise present in EM-based objective functions, due to which local search methods often fail to find the optimal design. While many commercial EM simulation packages have implemented basic design automation methods (mostly conventional gradient-based and derivative-free approaches such as Quasi-Newton or Nelder-Mead algorithms, or population-based algorithms such as genetic algorithms), a common practice is still to obtain satisfactory design using tedious and time-consuming parameter sweeps involving numerous full-wave EM simulations combined with engineering experience.

Efficient simulation-driven design can be performed using surrogate based optimization (SBO). The most successful SBO techniques in microwave engineering include space mapping (SM) (Bandler et al., 2004); (Koziel et al., 2008a); (Amari et al., 2006), simulation-based tuning (Swanson and Macchiarella, 2007); (Rautio, 2008), manifold mapping (MM) (Echeverria and Hemker, 2005), as well as shape-preserving response prediction (Koziel, 2010). While the SBO techniques can be extremely efficient, they are not straightforward to automate to make them reliable "push-button"-like approaches that could work for a variety of microwave problems. Their use typically requires some experience (Koziel et al., 2008a) and most of them are not globally convergent so that whether a satisfactory design is obtained or not may depend on a proper implementation, some parameter tuning, as well as certain knowledge particularly while constructing the surrogate model.

Another approach to improve efficiency of simulation-driven design is by using adjoint sensitivity that allows obtaining derivative information of the system of interest with little or no extra computational cost (Nair and Webb, 2003); (El Sabbagh et al., 2006); (Kiziltas et al., 2003); (Uchida et al., 2009); (Bakr et al., 2011). However, until recently, adjoint sensitivities were not commercially available, which means that they were not available for most engineers and designers. Situation changed a few years ago when

Koziel S., Leifsson L. and Ogurtsov S..
Microwave Design Optimization Exploiting Adjoint Sensitivity.
DOI: 10.5220/0004164104990506
In *Proceedings of the 2nd International Conference on Simulation and Modeling Methodologies, Technologies and Applications* (SDDOM-2012), pages 499-506
ISBN: 978-989-8565-20-4

adjoint sensitivities were implemented for instance in CST Microwave Studio (CST, 2011).

In this paper, we review several recent techniques that exploit adjoint sensivity in order to speed up the EM-simulation-driven microwave design process. These techniques include gradient-based search methods embedded in trust region framework, as well as surrogate-based methods, specifically space mapping (Koziel et al., 2008a) and manifold mapping (Echeverria and Hemker, 2005), enhanced by adjoint sensitivity in order to improve their convergence properties and reduce the computational cost of surrogate model optimization step. The efficiency of the presented approaches is demonstrated using several microwave design cases. A performance comparison with other optimization techniques, including Matlab's *fminimax* (Matlab, 2008) and a Quasi-Newton type of algorithm (Nocedal and Wright, 2000) is also provided.

2 DESIGN OPTIMIZATION WITH TRUST-REGION AND ADJOINT SENSITIVITIES

2.1 Design Problem Formulation

The microwave design task can be formulated as a nonlinear minimization problem

$$\boldsymbol{x}_f^* \in \arg\min_{\boldsymbol{x}} U\left(\boldsymbol{R}_f(\boldsymbol{x})\right) \tag{1}$$

where $\boldsymbol{R}_f \in R^m$ denotes the response vector of a high-fidelity (or fine) model of the microwave structure of interest evaluated through expensive high-fidelity EM simulation; $\boldsymbol{x} \in R^n$ is a vector of designable variables. Typically, these are geometry and/or material parameters. The response $\boldsymbol{R}_f(\boldsymbol{x})$ might be, e.g., the modulus of the transmission coefficient $|S_{21}|$ evaluated at m different frequencies. In some cases, $\boldsymbol{R}_f$ may consists of several vectors representing, e.g., filter reflection and transmission coefficients, or an antenna reflection, gain, etc. U is a given scalar merit function, e.g., a norm, or a minimax function with upper and lower specifications. U is formulated so that a better design corresponds to a smaller value of U. $\boldsymbol{x}_f^*$ is the optimal design to be determined.

Direct solution of (1) using conventional algorithm may be prohibitive because it usually requires a large number of fine model evaluations, each being computationally expensive by itself. For many structures, the evaluation time may be as long as a few hours.

2.2 Trust-Region-Based Optimization with Adjoint Sensitivity

The algorithm proposed in (Koziel et al., 2012a) uses the 1st-order model (or the surrogate) S(x) of the high-fidelity model Rf. S(i)(x) is nothing else but a linear function being a first-order Taylor expansion of Rf at x(i) of the form:

$$\begin{aligned}\boldsymbol{S}^{(i)}(\boldsymbol{x}, \boldsymbol{x}^{(i)}, \boldsymbol{R}_f(\boldsymbol{x}^{(i)}), J_{\boldsymbol{R}_f}(\boldsymbol{x}^{(i)})) &= \\ = \boldsymbol{R}_f(\boldsymbol{x}^{(i)}) + J_{\boldsymbol{R}_f}(\boldsymbol{x}^{(i)}) \cdot (\boldsymbol{x} - \boldsymbol{x}^{(i)})\end{aligned} \tag{2}$$

$J_{\boldsymbol{R}f}(\boldsymbol{x})$ is an estimated Jacobian of $\boldsymbol{R}_f$ at $\boldsymbol{x}$, $J_{\boldsymbol{R}f}(\boldsymbol{x}) = [\partial \boldsymbol{R}_{fi}/\partial x_j]_{i=1,\ldots,m;\, j=1,\ldots,n}$, obtained using adjoint sensitivity (if available) or finite differentiation $\partial \boldsymbol{R}_{fi}/\partial x_j \cong [\boldsymbol{R}_{fi}([x_1 \ldots x_j+d_j \ldots x_n]^T) - \boldsymbol{R}_{fi}(\boldsymbol{x})]/d_j$ for all the other parameters.

The optimization algorithm framework is the following (r_0 is the initial trust region radius)

1. $i = 0$; $r = r_0$;
2. Optimize a linear model: $\boldsymbol{x}_{tmp} = \text{argmin}\{\|\boldsymbol{x} - \boldsymbol{x}^{(i)}\| \le r : \boldsymbol{S}^{(i)}(\boldsymbol{x},\boldsymbol{x}^{(i)},\boldsymbol{R}_f(\boldsymbol{x}^{(i)}),J_F(\boldsymbol{x}^{(i)}))\}$;
3. Calculate gain ratio: $\rho = [U(\boldsymbol{R}_f(\boldsymbol{x}^{(i)}) - U(\boldsymbol{R}_f(\boldsymbol{x}_{tmp}))]/[U(\boldsymbol{R}_f(\boldsymbol{x}^{(i)}) - U(\boldsymbol{S}(\boldsymbol{x}_{tmp}))]$;
4. If $U(\boldsymbol{R}_f(x_{tmp})) < U(\boldsymbol{R}_f(x^{(i)}))$ then $\boldsymbol{x}^{(i+1)} = \boldsymbol{x}_{tmp}$; $i = i + 1$;
5. Update r: $\rho < r_{decr}$ then $r = r/m_{decr}$; else if $\rho > r_{incr}$ then $r = r \cdot m_{incr}$;
6. If termination condition is not satisfied, go to 2; else, END.

Here, r_{decr} and r_{incr} denote threshold values for decreasing or increasing the trust region radius by the corresponding factors m_{decr} and m_{incr}. The algorithm is terminated if either of the following conditions is satisfied: $r < \varepsilon_r$, $n_F < n_{Fmax}$, $\|\boldsymbol{x}^{(i)} - \boldsymbol{x}^{(i-1)}\| < \varepsilon_x$, or $\|U(\boldsymbol{R}_f(\boldsymbol{x}^{(i)})) - U(\boldsymbol{R}_f(\boldsymbol{x}^{(i-1)}))\| < \varepsilon_F$, where ε_r, ε_x, ε_F, n_{Fmax}, are user defined parameters, whereas n_F is the number of high-fidelity model evaluations.

The response Jacobian is recalculated after each successful iteration (i.e., when $U(\boldsymbol{R}_f(\boldsymbol{x}_{tmp})) < U(\boldsymbol{R}_f(\boldsymbol{x}^{(i)}))$) for those variables where adjoint sensitivity is available. The finite-difference sensitivity is not recalculated as long as the new iteration is successful in order to reduce the number of high fidelity function evaluations.

The above algorithm is a local-search method. Assuming that the exact sensitivity of Rf at x(i) is used to define the first-order model S(i), S(i) satisfies both zero- and first-order consistency conditions with the high-fidelity model Rf, i.e., S(i)(x(i)) = Rf(x(i)) and JS(x(i)) = JRf(x(i)). This is sufficient for the global convergence of the algorithm at least to a local optimum of the high-fidelity model, provided that Rf is sufficiently smooth (Alexandrov et al., 1998). In practice, the high-fidelity model is noisy, nevertheless, the performance of the algorithm is quite remarkable (Koziel et al., 2012a).

Responses obtained using EM solvers are inherently noisy (except, perhaps, when the mesh topology is fixed). The major reason is that the mesh topology is a discontinuous function of the design variables (or, more general, of geometry of the structure under considerations). The minor reason is that the evaluation process itself is noisy (e.g., due to finite tolerances used to terminate the EM simulation). This poses some problems for the optimization process. In particular, finite differentiation with conventional small increments (e.g., 10^{-8}) will not work: the value of the derivative obtained this way will be completely unreliable, regardless of the model discretization density. The reason is that the change of the response due to the small perturbation of any given design variable will be, most likely, much smaller than the amplitude of the numerical noise. For noisy functions, better and more consistent gradient estimation can be obtained using larger finite differentiation step sizes. Based on the above considerations, our algorithm uses relatively large steps for finite differentiation, typically, 10^{-3} or larger (depending on the absolute values of the design variables).

2.3 Example: Design of a Waveguide Bandpass Filter

Consider the waveguide filter shown in Fig. 1. Design variables are $[h_1\ h_2\ h_3\ s_1\ s_2\ s_3\ s_4\ w_1\ w_2\ w_3\ w_4]^T$. Design specifications are $|S_{11}| \le -20$ dB for 667.5 MHz $\le \omega \le$ 675 MHz. The initial design is $\boldsymbol{x}^{(0)}$ = [163.5 172 165.3 160.5 160.5 160.5 130.5 –60.5 –29.5 –28.5 –27.5]^T (minimax specification error +19.2 dB). Optimization results are shown in Table 1. Figure 2 shows the filter responses at the initial design and at the optimized design found by the algorithm of Section 2.2. In this case, the proposed algorithm performs substantially better than the methods used for comparison both with respect to the computational cost of the design process and the quality of the final design. It should be noted that the computational complexity of our algorithm using finite-differences derivatives is comparable to that of Matlab's *fminimax*, even though the latter exploits adjoint sensitivity.

3 SURROGATE-BASED OPTIMIZATION WITH ADJOINT SENSITIVITY

3.1 Surrogate-based Optimization

A generic surrogate-based optimization (SBO) algorithm (Koziel and Yang, 2011); (Forrester and Keane, 2009) generates a sequence of approximate solutions to (1), $\boldsymbol{x}^{(i)}$, as follows

$$\boldsymbol{x}^{(i+1)} = \arg\min_{\boldsymbol{x}} U\left(\boldsymbol{R}_s^{(i)}(\boldsymbol{x})\right) \qquad (3)$$

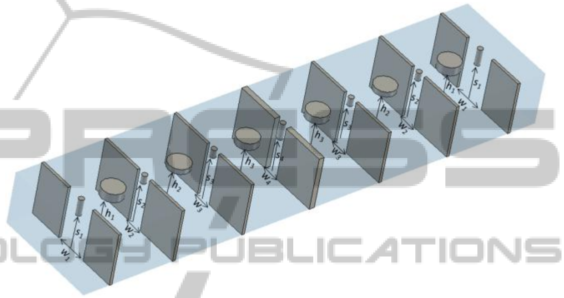

Figure 1: Geometry of a waveguide bandpass filter.

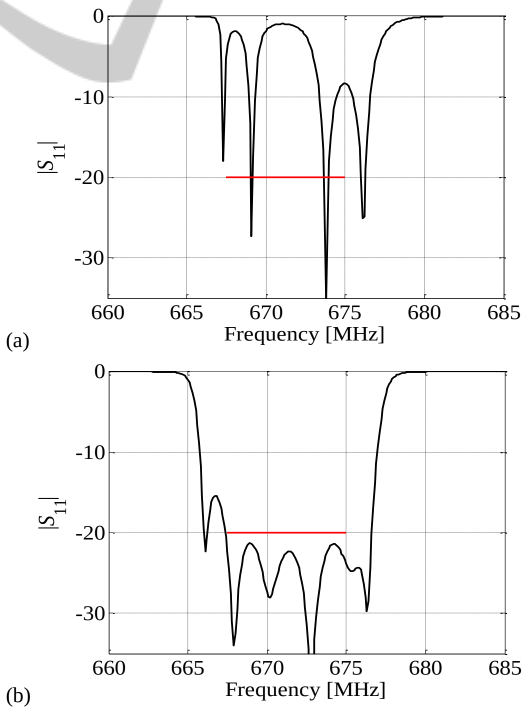

Figure 2: Waveguide bandpass filter: (a) responses at the initial design $\boldsymbol{x}^{(0)}$; (b) responses at the optimized design found by the proposed algorithm using mixed adjoint and finite-difference sensitivities.

Table 1: Optimization results for the waveguide bandpass filter.

Optimization Algorithm		Final Specification Error	Number of Function Evaluations
Quasi-Newton optimizer		+5.3 dB	1454
Matlab's *fminimax*		+1.2 dB	88
This work (Algorithm of Section 2)	Adjoint sensitivity	–2.2 dB	16
	Mixed adjoint / finite-difference sensitivity*	–1.3 dB	46
	Finite-difference sensitivity	–0.4 dB	107

* Adjoint sensitivity for the first seven variables, finite-differences for the remaining four variables.

where $\boldsymbol{R}_s^{(i)}$ is the surrogate model at iteration *i*. Here, $\boldsymbol{x}^{(0)}$ is the initial design. $\boldsymbol{R}_s^{(i)}$ is assumed to be a computationally cheap and sufficiently reliable representation of $\boldsymbol{R}_f$, particularly in the neighborhood of $\boldsymbol{x}^{(i)}$. Under these assumptions, the algorithm (3) is likely to produce a sequence of designs that quickly approach $\boldsymbol{x}_f^*$. Usually, $\boldsymbol{R}_f$ is only evaluated once per iteration (at every new design $\boldsymbol{x}^{(i+1)}$) for verification purposes and to obtain the data necessary to update the surrogate model. Because of the low computational cost of the surrogate model, its optimization cost can usually be neglected and the total optimization cost is determined by the evaluation of $\boldsymbol{R}_f$. The key point here is that the number of evaluations of $\boldsymbol{R}_f$ for a well performing surrogate-based algorithm is substantially smaller than for most conventional optimization methods.

3.2 Robustness of SBO Algorithms

Robustness of the surrogate-based optimization process (3) depends on the quality of the surrogate model $\boldsymbol{R}_s^{(i)}$. In general, in order to ensure convergence of the algorithm (3) to at least local optimum of the high-fidelity model, the first-order consistency conditions have to be met (Alexandrov and Lewis, 2001), i.e., one has to have $\boldsymbol{R}_s^{(i)}(\boldsymbol{x}^{(i)}) = \boldsymbol{R}_f(\boldsymbol{x}^{(i)})$ and $\boldsymbol{J}_{\boldsymbol{R}_s^{(i)}}(\boldsymbol{x}^{(i)}) = \boldsymbol{J}_{\boldsymbol{R}_f}(\boldsymbol{x}^{(i)})$, where $\boldsymbol{J}$ stands for the Jacobian of the respective model. Also, the process (3) has to be embedded in the trust-region (TR) framework (Conn *et al.*, 2000), i.e., we have

$$\boldsymbol{x}^{(i+1)} = \arg \min_{\boldsymbol{x}:\|\boldsymbol{x}-\boldsymbol{x}^{(i)}\| \le \delta^{(i)}} U(\boldsymbol{R}_s^{(i)}(\boldsymbol{x})) \quad (4)$$

where the TR radius $\delta^{(i)}$ is updated using classical rules (Conn et al., 2000). In general, the SBO algorithm (4) can be successfully utilized without satisfying the aforementioned conditions, see, e.g. (Bandler et al., 2004); (Koziel et al., 2008a). However, in these cases, the quality of the underlying low-fidelity model may be critical for performance (including the algorithm convergence) (Koziel et al., 2008b) and accurate location of the optimum design may not be possible.

Availability of cheap adjoint sensitivity (Nair and Webb, 2003); (CST, 2011) makes it possible to satisfy consistency conditions in a easy way (without excessive computational cost by using, e.g., finite differentiation). A few options exploiting this possibility are discussed in the next section.

3.3 SBO with First-order Taylor Model and Trust Regions

The simplest way of exploring adjoint sensitivity for antenna optimization is to use the following surrogate model for the SBO scheme (4):

$$\boldsymbol{R}_s^{(i)}(\boldsymbol{x}) = \boldsymbol{R}_f(\boldsymbol{x}^{(i)}) + \boldsymbol{J}_{\boldsymbol{R}_f}(\boldsymbol{x}^{(i)}) \cdot (\boldsymbol{x} - \boldsymbol{x}^{(i)}) \quad (5)$$

where $\boldsymbol{J}_{\boldsymbol{R}f}$ is the Jacobian of $\boldsymbol{R}_f$ obtained using adjoint sensitivity technique. The key point of the algorithm is finding the new design $\boldsymbol{x}^{(i)}$ and the updating process for the search radius $\delta^{(i)}$. Here, instead of the standard rules, we use the following strategy ($\boldsymbol{x}^{(i-1)}$ and $\delta^{(i-1)}$ are the previous design and the search radius, respectively):

1. For $\delta_k = k \cdot \delta^{(i-1)}$, $k = 0, 1, 2$, solve: $\boldsymbol{x}^k = \arg \min_{\boldsymbol{x}:\|\boldsymbol{x}-\boldsymbol{x}^{(i)}\| \le \delta_k} U(\boldsymbol{R}_s^{(i)}(\boldsymbol{x}))$. Note that $\boldsymbol{x}^0 = \boldsymbol{x}^{(i-1)}$. The values of δ_k and $U_k = U(\boldsymbol{R}_s^{(i)}(\boldsymbol{x}^k))$ are interpolated using 2nd-order polynomial to find δ^* that gives the smallest (estimated) value of the specification error (δ^* is limited to $3 \cdot \delta^{(i-1)}$). Set $\delta^{(i)} = \delta^*$.
2. Find a new design $\boldsymbol{x}^{(i)}$ by solving (4) with the current $\delta^{(i)}$.
3. Calculate the gain ratio $\rho = [U(\boldsymbol{R}_f(\boldsymbol{x}^{(i)})) - U_0]/[U(\boldsymbol{R}_s^{(i)}(\boldsymbol{x}^{(i)})) - U_0]$; If $\rho < 0.25$ then $\delta^{(i)} = \delta^{(i)}/3$; else if $\rho > 0.75$ then $\delta^{(i)} = 2 \cdot \delta^{(i)}$;
4. If $\rho < 0$ go to 2;
5. Return $\boldsymbol{x}^{(i)}$ and $\delta^{(i)}$;

The trial points $\boldsymbol{x}^k$ are used to find the best value of the search radius, which is further updated based on the gain ratio ρ (actual versus expected objective function improvement). If the new design is worse than the previous one, the search radius is reduced to find $\boldsymbol{x}^{(i)}$ again, which eventually will bring the improvement of U as $\boldsymbol{R}_s^{(i)}$ and $\boldsymbol{R}_f$ are first-order consistent (Alexandrov and Lewis, 2001). This precaution is necessary because the procedure in Step 1 only gives an estimation of the search radius.

As an example, consider a wideband hybrid antenna (Petosa, 2007) shown in Fig. 3, a quarter-wavelength monopole loaded by dielectric ring resonator. The design goal is to have $|S_{11}| \leq -20$ dB for 8-to-13 GHz. The design variables are $\boldsymbol{x} = [h_1\ h_2\ r_1\ r_2\ g]^T$. The initial design is $\boldsymbol{x}^{(0)} = [2.5\ 9.4\ 2.3\ 3.0\ 0.5]^T$ mm. Other parameters are fixed. The final design with the proposed algorithm is $\boldsymbol{x}^{(0)} = [3.94\ 10.01\ 2.23\ 3.68\ 0.0]^T$ mm. Table 2 and Fig. 4 compare the design cost and quality of the final design found by the algorithm described above and Matlab's *fminimax*. It can be observed that our algorithm yields better design at significantly smaller computational cost (75 percent design time reduction).

3.4 Space Mapping and Manifold Mapping

Construction of the surrogate model can also be based on the underlying low-fidelity (or coarse) model $\boldsymbol{R}_c$, e.g., obtained from coarse-discretization EM simulation data. The two methods considered here that use this approach are space mapping (SM) (Koziel et al., 2008a) and manifold mapping (MM) (Echeverria and Hemker, 2005). Usually, the knowledge about the system embedded in the low-fidelity model allows us to reduce the number of high-fidelity model evaluations necessary to find an optimum design.

The SM surrogate considered here is constructed using input and output SM (Bandler *et al.*, 2004) of the form:

$$\boldsymbol{R}_s^{(i)}(\boldsymbol{x}) = \boldsymbol{R}_c(\boldsymbol{x}+\boldsymbol{c}^{(i)}) + \boldsymbol{d}^{(i)} + \boldsymbol{E}^{(i)}(\boldsymbol{x}-\boldsymbol{x}^{(i)}) \quad (6)$$

Here, only the input SM vector $\boldsymbol{c}^{(i)}$ is obtained through the nonlinear parameter extraction process

$$\boldsymbol{c}^{(i)} = \arg\min_{\boldsymbol{c}} \| \boldsymbol{R}_f(\boldsymbol{x}^{(i)}) - \boldsymbol{R}_c(\boldsymbol{x}^{(i)}+\boldsymbol{c}) \| \quad (7)$$

Output SM parameters are calculated as

$$\boldsymbol{d}^{(i)} = \boldsymbol{R}_f(\boldsymbol{x}^{(i)}) - \boldsymbol{R}_c(\boldsymbol{x}^{(i)}+\boldsymbol{c}^{(i)}) \quad (8)$$

and

$$\boldsymbol{E}^{(i)} = \boldsymbol{J}_{\boldsymbol{R}_f}(\boldsymbol{x}^{(i)}) - \boldsymbol{J}_{\boldsymbol{R}_c}(\boldsymbol{x}^{(i)}+\boldsymbol{c}^{(i)}) \quad (9)$$

Formulation (6)-(9) ensures zero- and first-order consistency (Alexandrov and Lewis, 2001) between the surrogate and the fine model.

The manifold mapping (MM) surrogate model is defined as (Echeverria and Hemker, 2005)

$$\boldsymbol{R}_s^{(i)}(\boldsymbol{x}) = \boldsymbol{R}_f(\boldsymbol{x}^{(i)}) + \boldsymbol{S}^{(i)}\left(\boldsymbol{R}_c(\boldsymbol{x}) - \boldsymbol{R}_c(\boldsymbol{x}^{(i)})\right) \quad (10)$$

where $\boldsymbol{S}^{(i)}$ is the $m\times m$ correction matrix defined as

$$\boldsymbol{S}^{(i)} = \boldsymbol{J}_{\boldsymbol{R}_f}(\boldsymbol{x}^{(i)}) \cdot \boldsymbol{J}_{\boldsymbol{R}_c}(\boldsymbol{x}^{(i)})^{\dagger} \quad (11)$$

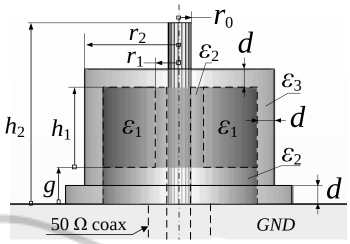

Figure 3: Wideband hybrid antenna: geometry.

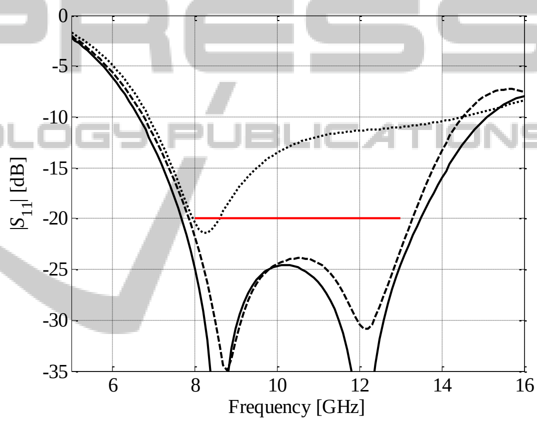

Figure 4: Wideband hybrid antenna: reflection response at the initial design (· · ·), at the final design by Matlab's *fminimax* (- - -), and by the proposed algorithm (—).

Table 2: Wideband hybrid antenna: design results.

Algorithm	max$\|S_{11}\|$ for 8 to 13 GHz at Final Design	Design Cost (Number of EM Analyses)
Matlab's *fminimax*	–22.6 dB	98
This work	–24.6 dB	24

The pseudoinverse, denoted by †, is defined as

$$\boldsymbol{J}_{\boldsymbol{R}_c}{}^{\dagger} = \boldsymbol{V}_{J_{R_c}} \boldsymbol{\Sigma}_{J_{R_c}}^{\dagger} \boldsymbol{U}_{J_{R_c}}^{T} \quad (12)$$

where $\boldsymbol{U}_{\boldsymbol{J}\boldsymbol{R}c}$, $\Sigma_{\boldsymbol{J}\boldsymbol{R}c}$, and $\boldsymbol{V}_{\boldsymbol{J}\boldsymbol{R}c}$ are the factors in the singular value decomposition of $\boldsymbol{J}_{\boldsymbol{R}c}$. The matrix $\boldsymbol{\Sigma}_{\boldsymbol{J}\boldsymbol{R}c}{}^{\dagger}$ is the result of inverting the nonzero entries in $\boldsymbol{\Sigma}_{\boldsymbol{J}\boldsymbol{R}c}$, leaving the zeroes invariant (Echeverria and Hemker, 2005). Using the sensitivity data as in (12) ensures that the surrogate model (10) is first-order consistent with the fine model. In our implementation, the coarse model is preconditioned using input space mapping of the form (7) in order to improve its initial alignment with the fine model.

Both the parameter extraction (7) and surrogate model optimization processes (4) are implemented by exploiting adjoint sensitivity data of the low-fidelity model, which allows for further cost savings. The details of these implementations can be found in (Koziel et al., 2012b).

In order to illustrate the operation and performance of the SM and MM algorithms, let us consider an UWB antenna shown in Fig. 5. The antenna and its models include: a microstrip monopole, housing, edge mount SMA connector, section of the feeding coax. The design variables are $\boldsymbol{x} = [l_1\ l_2\ l_3\ w_1]^T$. Simulation time of the low-fidelity model $\boldsymbol{R}_c$ (156,000 mesh cells) is 1 min, and that of the high-fidelity model $\boldsymbol{R}_f$ (1,992,060 mesh cells) is 40 min (both at the initial design). Both models are simulated with the transient solver of CST Microwave Studio (CST, 2011). The design specifications for reflection are $|S_{11}| \leq -12$ dB for 3.1 GHz to 10.6 GHz. The initial design is $\boldsymbol{x}^{init} = [20\ 2\ 0\ 25]^T$ mm.

The antenna was optimized using the SBO algorithm (4) with both the SM and MM surrogate models. Fig. 6(a) shows the responses of $\boldsymbol{R}_f$ and $\boldsymbol{R}_c$ at $\boldsymbol{x}^{init}$. Fig. 6(b) shows the response of the high-fidelity model at the final design $\boldsymbol{x}^{(2)} = [20.22\ 2.43\ 0.128\ 19.48]^T$ ($|S_{11}| \leq -12.5$ dB for 3.1 to 10.6 GHz) obtained after only two SBO iterations with MM surrogate, i.e. only 4 evaluations of the high-fidelity model (Table 3). The number of function evaluations is larger than the number of MM iterations because some designs can be rejected by the TR mechanism. The algorithm using SM surrogate required three iterations and the final design is $\boldsymbol{x}^{(3)} = [20.29\ 2.27\ 0.058\ 19.63]^T$ ($|S_{11}| \leq -12.8$ dB for 3.1 to 10.6 GHz) obtained after three SM iterations. The total optimization cost (Table 4) is equivalent to around 6 evaluations of the fine model. Figure 7 shows the evolution of the specification algorithm for the manifold mapping algorithm.

As another example, consider the third-order Chebyshev bandpass filter (Kuo et al., 2003) shown in Fig. 8. The design variables are $\boldsymbol{x} = [L_1\ L_2\ S_1\ S_2]^T$ mm. Other parameters are: $W_1 = W_2 = 0.4$ mm. Both fine (396,550 mesh cells, evaluation time 45 min) and coarse (82,350 mesh cells, evaluation time 1 min) models are evaluated by the CST MWS transient solver (CST, 2011).

The design specifications are $|S_{21}| \geq -3$ dB for $1.8\text{ GHz} \leq \omega \leq 2.2$ GHz, and $|S_{21}| \leq -20$ dB for $1.0\text{ GHz} \leq \omega \leq 1.55$GHz and $2.45\text{ GHz} \leq \omega \leq 3.0$ GHz. The initial design is the coarse model optimal solution $\boldsymbol{x}^{init} = [16\ 16\ 1\ 1]^T$ mm.

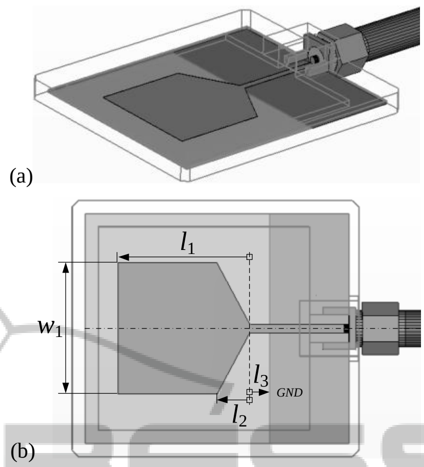

Figure 5: UWB monopole: (a) 3D view; (b) top view. The housing is shown transparent.

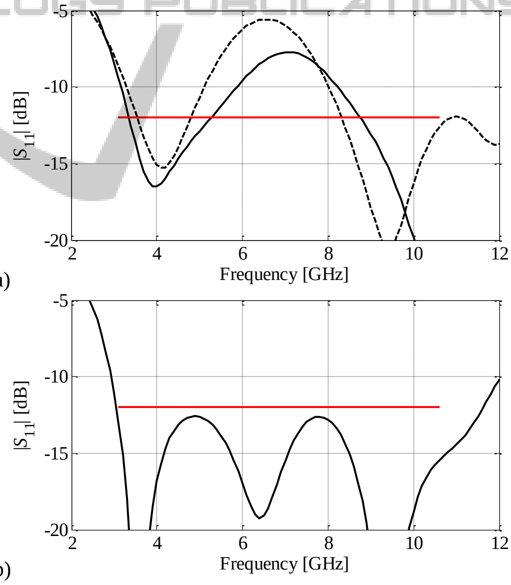

Figure 6: UWB monopole optimized using manifold mapping algorithm: (a) responses of $\boldsymbol{R}_f$ (—) and $\boldsymbol{R}_c$ (- - -) at the initial design $\boldsymbol{x}^{init}$; (b) response of $\boldsymbol{R}_f$ (—) at the final design.

The filter was optimized using the SM algorithm. Optimization results are shown in Fig. 9 and Table 5. The final design $\boldsymbol{x}^{(5)} = [14.58\ 14.57\ 0.93\ 0.56]^T$ is obtained after five SM iterations. As before, optimization cost is very low. Also, thanks to sensitivity information as well as trust region, the algorithm improves the specification error at each iteration, see Fig. 10. This is not the case for conventional space mapping (Bandler et al., 2004).

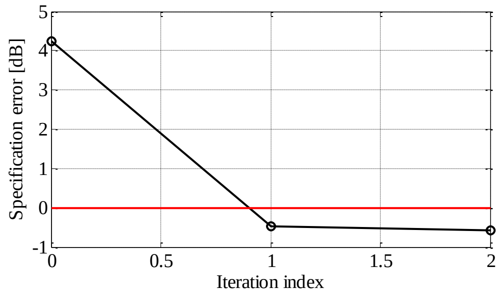

Figure 7: UWB monopole: Minimax specification error versus manifold mapping algorithm iteration index.

Table 3: UWB monopole antenna: optimization results using manifold mapping.

Algorithm Component	Number of Model Evaluations*	CPU Time	
		Absolute	Relative to R_f
Evaluation of R_c	31	31 min	0.8
Evaluation of R_f	4	120 min	4.0
Total cost*	N/A	151 min	**4.8**

* Includes R_f evaluation at the initial design.

Table 4: UWB monopole antenna: optimization results using space mapping.

Algorithm Component	Number of Model Evaluations*	CPU Time	
		Absolute	Relative to R_f
Evaluation of R_c	45	45 min	1.1
Evaluation of R_f	5	200 min	5.0
Total cost*	N/A	205 min	**6.1**

* Includes R_f evaluation at the initial design.

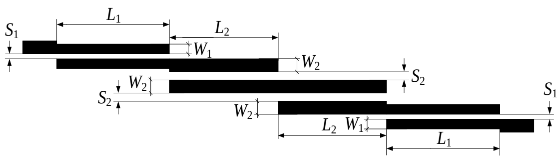

Figure 8: Third-order Chebyshev bandpass filter: geometry.

4 CONCLUSIONS

A review of recent microwave design optimization techniques exploiting adjoint sensitivity has been presented. We have demonstrated that by exploiting cheap derivative information, the EM-simulation-driven design process can be performed efficiently and in a robust way. Adjoint sensitivity can also be used to improve performance of the surrogate-based optimization algorithm as illustrated on the example of space mapping and manifold mapping techniques.

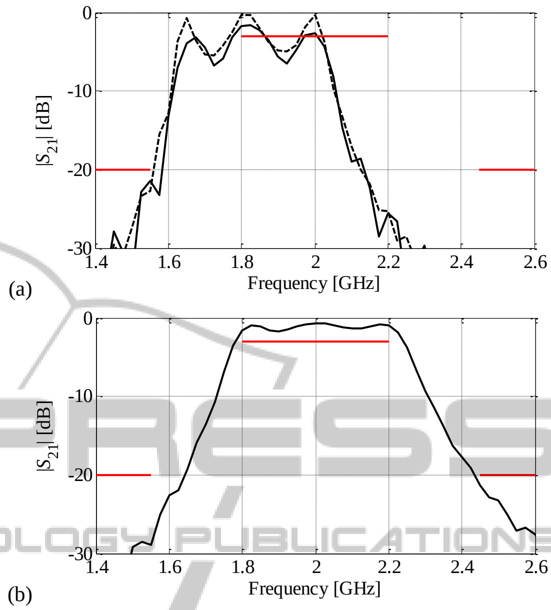

Figure 9: Third-order Chebyshev filter: (a) responses of R_f (—) and R_c (- - -) at the initial design x^{init}; (b) response of R_f (—) at the final design.

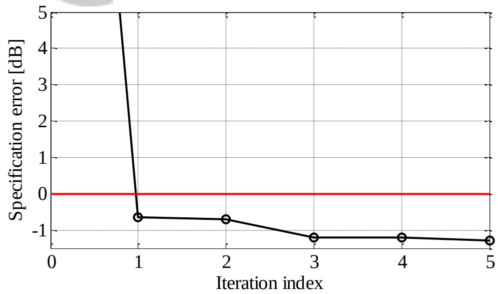

Figure 10: Third-order Chebyshev filter: minimax specification error versus SM iteration index.

Table 5: Third-order Chebyshev filter: optimization results using space mapping.

Algorithm Component	Number of Model Evaluations*	CPU Time	
		Absolute	Relative to R_f
Evaluation of R_c	67	67 min	1.5
Evaluation of R_f	6	270 min	6.0
Total cost*	N/A	337 min	**7.5**

* Includes R_f evaluation at the initial design.

ACKNOWLEDGEMENTS

The authors would like to thank CST AG for making CST Microwave Studio available. This work was supported in part by the Icelandic Centre for Research (RANNIS) Grant 110034021.

REFERENCES

Alexandrov, N. M., Dennis, J. E., Lewis, R. M., Torczon, V., 1998. A trust region framework for managing use of approximation models in optimization. *Struct. Multidisciplinary Optim.*, vol. 15, no. 1, pp. 16-23.

Alexandrov, N. M., Lewis, R. M., 2001, An overview of first-order model management for engineering optimization. *Optimization Eng.*, vol. 2, no. 4, pp. 413-430.

Amari, S., LeDrew, C., Menzel, W., 2006. Space-mapping optimization of planar coupled-resonator microwave filters. *IEEE Trans. Microwave Theory Tech.*, vol. 54, no. 5, pp. 2153-2159.

Bakr, M. H., Ghassemi, M., Sangary, N., 2011, Bandwidth enhancement of narrow band antennas exploiting adjoint-based geometry evolution. *IEEE Int. Symp. Antennas Prop.*, pp. 2909-2911.

Bandler, J. W., Cheng, Q. S., Dakroury, S. A., Mohamed, A. S., Bakr, M. H., Madsen, K., Søndergaard, J., 2004. Space mapping: the state of the art. *IEEE Trans. Microwave Theory Tech.*, vol. 52, no. 1, pp. 337-361.

Conn, A. R., Gould, N. I. M., Toint, P. L., 2000. *Trust Region Methods*, MPS-SIAM Series on Optimization.

CST MICROWAVE STUDIO®, 2011, CST AG, Bad Nauheimer Str. 19, D-64289 Darmstadt, Germany.

El Sabbagh, M. A., Bakr, M. H., Nikolova, N. K., 2006, Sensitivity analysis of the scattering parameters of microwave filters using the adjoint network method. *Int. J. RF and Microwave Computer-Aided Eng.*, vol. 16, no. 6, pp. 596-606.

Echeverria, D., Hemker, P. W., 2005. Space mapping and defect correction. *CMAM The International Mathematical Journal Computational Methods in Applied Mathematics.* vol. 5, no. 2, pp. 107-136.

Forrester, A. I .J., Keane, A. J., 2009. Recent advances in surrogate-based optimization, *Prog. in Aerospace Sciences*, vol. 45, no. 1-3, pp. 50-79.

Kiziltas, G., Psychoudakis, D., Volakis, J. L., Kikuchi, N., 2003, Topology design optimization of dielectric substrates for bandwidth improvement of a patch antenna. *IEEE Trans. Antennas Prop*., vol. 51, no. 10, pp. 2732-2743.

Koziel, S., Cheng, Q. S., Bandler, J. W., 2008a. Space mapping. *IEEE Microwave Magazine*, vol. 9, no. 6, pp. 105-122.

Koziel, S., Bandler, J. W., Madsen, K., 2008b, Quality assessment of coarse models and surrogates for space mapping optimization. *Optimization and Engineering*, vol. 9, no. 4, pp. 375-391.

Koziel, S., 2010. Shape-preserving response prediction for microwave design optimization. *IEEE Trans. Microwave Theory and Tech.*, vol. 58, no. 11, pp. 2829-2837.

Koziel, S., Yang, X. S., (Eds.), 2011, Computational optimization, methods and algorithms, *Series: Studies in Computational Intelligence*, vol. 356, Springer.

Koziel, S., Mosler, F., Reitzinger, S., Thoma, P., 2012a, Robust microwave design optimization using adjoint sensitivity and trust regions. *Int. J. RF and Microwave CAE*, vol. 22, no. 1, pp. 10-19.

Koziel, S., Ogurtsov, S., Bandler, J. W., Cheng, Q. S., 2012b, Robust space mapping optimization exploiting EM-based models with adjoint sensitivity. *IEEE MTT-S Int. Microwave Symp. Dig*.

Kuo, J. T., Chen, S. P., Jiang, M., 2003, Parallel-coupled microstrip filters with over-coupled end stages for suppression of spurious responses. *IEEE Microwave and Wireless Comp. Lett.*, vol. 13, no. 10, pp. 440-442.

Matlab™, Version 7.6, 2008, The MathWorks, Inc., 3 Apple Hill Drive, Natick, MA 01760-2098.

Nair, D., Webb, J. P., 2003, Optimization of microwave devices using 3-D finite elements and the design sensitivity of the frequency response. *IEEE Trans. Magn.*, vol. 39, no. 3, pp. 1325-1328.

Nocedal, J., Wright, S. J., 2000, *Numerical Optimization*, Springer Series in Operations Research, Springer.

Petosa, A., 2007. *Dielectric Resonator Antenna Handbook*, Artech House.

Rautio, J. C., 2008. Perfectly calibrated internal ports in EM analysis of planar circuits. *IEEE MTT-S Int. Microwave Symp. Dig.*, Atlanta, GA, pp. 1373-1376.

Swanson, D. Macchiarella, G., 2007, Microwave filter design by synthesis and optimization. *IEEE Microwave Magazine*, vol. 8, no. 2, pp. 55-69.

Uchida, N., Nishiwaki, S., Izui, K., Yoshimura, M., Nomura, T., Sato, K., 2009, Simultaneous shape and topology optimization for the design of patch antennas. *European Conf. Antennas Prop.*, pp. 103 – 107.